Carbon-Coated V2O5 Nanocrystals as High Performance Cathode Material for Lithium Ion Batteries

ARTICLE *in* CHEMISTRY OF MATERIALS · DECEMBER 2011

Impact Factor: 8.35 · DOI: 10.1021/cm202812z

4 AUTHORS, INCLUDING:

Xiaofei Zhang
University of Münster
6 PUBLICATIONS **141** CITATIONS
SEE PROFILE

Kaixue Wang
Shanghai Jiao Tong University
103 PUBLICATIONS **2,810** CITATIONS
SEE PROFILE

CHEMISTRY OF MATERIALS

Communication

pubs.acs.org/cm

Carbon-Coated V_2O_5 Nanocrystals as High Performance Cathode Material for Lithium Ion Batteries

Xiao-Fei Zhang, Kai-Xue Wang,* Xiao Wei, and Jie-Sheng Chen*

School of Chemistry and Chemical Engineering, Shanghai Jiao Tong University, 800 Dongchuan Road, Shanghai 200240, China.

Supporting Information

KEYWORDS: *V_2O_5 nanocrystals, lithium ion batteries, porous carbon*

Rechargeable lithium ion batteries have been extensively exploited as energy storage devices for electric, hybrid electric vehicles, and intermittent renewable energy sources because of their high energy and power densities and long cycle lifetime.[1,2] The successful adoption of lithium ion batteries for transportation and stationary electric energy storage largely relies on the factors such as cost, safety, cycleability, and power and energy densities of the electrode materials. A variety of compounds have been tested, and some of them have been used commercially as cathode materials for the manufacture of lithium ion batteries. Among the compounds tested so far is V_2O_5, the crystal structure of which is formed by the stacking of V_2O_5 layers perpendicular to the *c*-axis via van der Waals interaction. Because of the layer structure feature of V_2O_5, the intercalation of guest species such as lithium ions into this oxide compound is quite feasible. In addition, vanadium is abundant in the crust of Earth, guaranteeing the availability and low cost of V_2O_5. Since the mid-1970s, V_2O_5 has been vigorously investigated as an electrode material because of its high capacity, high output voltage, and low cost.[3] However, bulk V_2O_5 suffers from poor rate capability and cycleability due to its low diffusion coefficient of lithium ions, slow electron conductivity, and the irreversible phase transitions upon deep discharge,[4−12] making the general application of V_2O_5 in lithium ion batteries greatly limited.

The rate capability of electrode materials is mainly determined by the kinetics of lithium-ion diffusion and electronic conductivity. Lithium-ion diffusion in the lattice of an electrode is associated with the lithium-ion diffusion coefficient and the diffusion length.[13] For a given electrode material, the diffusion coefficient is a constant. Thus, the decrease in diffusion distance can effectively shorten the diffusion time of lithium ions within the electrode. Nanomaterials can provide shortened diffusion paths of lithium ions during insertion/extraction, resulting in enhanced rate capability.[14−16] The transportation of electrons within the electrode also exerts a significant impact on the rate capability of lithium-ion batteries. The resistance arising from the low electronic conductivity of the electrode materials and the particle−particle interfaces is unfavorable for electron transportation. Surface coating of electrode particles with a highly conductive substance (such as carbon) can facilitate the electron transportation in the electrode. Moreover, the surface coating may restrain the surface reactions and the volume change upon lithium-ion insertion/extraction,[17] ensuring better cycleability during long-term charge/discharge. Thus, decreases in particle size and surface coating by conductive substance are thought to be effective approaches for enhancing rate capability and cycleability of V_2O_5 materials. However, to date, the efforts in these two aspects have not seen much success for the preparation of high performance V_2O_5 cathode materials for Li-ion batteries. In this communication, we describe the preparation of carbon-coated V_2O_5 nanocrystals via a unique capillary-induced filling strategy. The nanocrystals we obtained exhibit markedly enhanced rate capability and excellent cycleability when used as a cathode material for Li-ion batteries.

The carbon-coated V_2O_5 nanocrystals were achieved using porous carbon[18] as a hard template via a route illustrated in Scheme 1. First, mesoporous carbonaceous monoliths were prepared through a thermopolymerization process at low temperatures from a resol precursor in ethanol. The subsequent pyrolysis of the carbonaceous monoliths at a temperature of 800 °C under nitrogen led to the formation of mesoporous carbon. The resultant mesoporous carbon and V_2O_5 were mixed and heated in a vacuum at a temperature of 750 °C. Because the melting point of V_2O_5 is 690 °C, it was very easy for the oxide compound to become molten at 750 °C. Once the V_2O_5 was molten, the strong capillary force drove the compound into the pores of the carbon template, leading to the formation of a mesostructured carbon-V_2O_5 composite (see Figures S1 and S2 in the Supporting Information). Carbon-

Scheme 1. Schematic Formation of Carbon-Coated V_2O_5 Nanocrystals Using Mesoporous Carbon as a Template

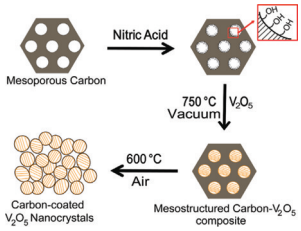

Received: September 19, 2011
Revised: November 18, 2011
Published: November 29, 2011

coated V_2O_5 nanoparticles were obtained by removing the majority of the carbon species from the as-formed carbon-V_2O_5 composite at 600 °C in air. A detailed preparation procedure of the final product is presented in the Supporting Information.

On the basis of the nitrogen adsorption/desorption measurements at 77 K, the Brunauer–Emmett–Teller (BET) surface areas of the mesoporous carbon and the carbon-V_2O_5 composite are 1048 and 382 m^2/g, respectively. The mesoporous carbon has an average pore diameter of approximately 3.8 nm, while the carbon-V_2O_5 composite has a broad pore size distribution centered at about 2.1 nm. The distinct decrease in surface area and average pore diameter suggest that most of the carbon mesopores in the composite are occupied by V_2O_5. The BET surface area of the V_2O_5 nanocrystals obtained through removal of the mesoporous carbon at 600 °C in air is only 11 m^2/g.

The morphology and crystal structure of the as-prepared material are examined by transmission electron microscopy

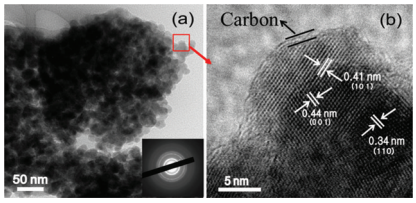

Figure 1. (a) TEM and (b) high resolution TEM images of V_2O_5 nanocrystals, showing the dimension, carbon coating, and high crystallinity of the material. Inset: the corresponding selected area electron diffraction (SAED) pattern.

(TEM) (Figure 1). V_2O_5 nanocrystals with particle sizes ranging from 10 to 20 nm aggregate together to form larger secondary particles with a diameter of several hundred nanometers. Although mesoporous carbon is employed as a hard template, no regular ordered mesoporous structure of V_2O_5 is observed in the final product. It is noted that the incorporation of V_2O_5 in a vacuum at 750 °C does not damage the well-ordered mesoporous structure of the hard template, as demonstrated in the TEM image (see the Supporting Information). Only after the subsequent calcination at 600 °C in air does the ordered mesostructure disappear, accompanied by the decomposition of the carbon walls and crystal growth of V_2O_5. The growth of V_2O_5 nanocrystals eliminates a substantial part of the voids left by the carbon removal, but plenty of interparticle voids are still present (Figure 1a). As revealed by high resolution TEM (HRTEM), a thin carbon layer with a thickness less than 2 nm covers the surface of the V_2O_5 particles. The carbon coating is formed during the decomposition of the mesoporous carbon template at 600 °C for approximately 45 min. Elemental analysis shows that the carbon content of the composite material is approximately 0.15 wt %. The HRTEM image (Figure 1b) shows lattice fringes with regular spacings of 0.44, 0.41, and 0.34 nm associated with the (001), (101), and (110) planes of V_2O_5, respectively. The well resolved fringes indicate the high crystallinity of the V_2O_5 nanocrystals, which is confirmed by powder X-ray diffraction (XRD) (see Figure S3 in the Supporting Information). The peaks well correspond to orthorhombic V_2O_5 (JCPDS No. 41-1426, space group *Pmnm*; a = 11.52, b = 3.57, and c = 4.37 Å).

Cyclic voltammograms (CV) of the carbon-coated V_2O_5 nanocrystals were measured at a scan rate of 1.0 mV/s in the

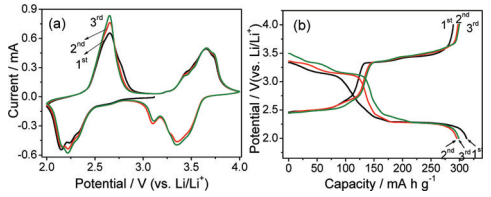

Figure 2. (a) Cyclic voltammograms at a scan rate of 1.0 mV/s and (b) the first three discharge–charge profiles recorded at 1.0 A/g for the carbon-coated V_2O_5.

potential range from 4.0 to 2.0 V (vs Li/Li^+) at room temperature (Figure 2a). The cathodic and anodic peaks are ascribed to the lithium ion insertion and extraction processes for the electrode, respectively. Three main cathodic peaks appear at potentials of 3.4, 3.1, and 2.2 V (vs Li/Li^+) in the CV curves, corresponding to the phase transformations from α-V_2O_5 to ε-$Li_{0.5}V_2O_5$, δ-LiV_2O_5, and γ-$Li_2V_2O_5$, respectively. In the subsequent scans, the shapes of the curves are almost identical, indicative of good reversibility for the carbon-coated V_2O_5 nanocrystals upon polarization to a voltage as low as 2 V (vs Li/Li^+). The cathodic performance of carbon-coated V_2O_5 nanocrystals was evaluated by galvanostatic discharge/charge testing. Figure 2b shows the first three cycles of discharge (Li insertion) and charge (Li extraction) curves of the V_2O_5 electrode in the voltage window of 2.0 − 4.0 V at a current density of 1.0 A g^{-1} (rate of approximately 6.8C), consistent with the CV scans. Multiple voltage plateaus due to different redox reactions associated with Li insertion are clearly observed in the discharge curves. The first two plateaus at approximately 3.4 and 3.2 V are ascribed to the phase transitions from α-V_2O_5 to ε-$Li_{0.5}V_2O_5$ and δ-LiV_2O_5, corresponding to eqs 1 and 2, respectively. The combined discharge capacity related to these phase transitions is over 140 mAh g^{-1}, consistent with the theoretical value of 147 mAh g^{-1} for the formation of δ-LiV_2O_5. The plateau at approximately 2.3 V is attributed to the generation of γ-$Li_2V_2O_5$, resulting from further lithium insertion into LiV_2O_5 (eq 3).

$$V_2O_5 + 0.5Li^+ + 0.5e^- = \varepsilon\text{-}Li_{0.5}V_2O_5 \quad (1)$$

$$\varepsilon\text{-}Li_{0.5}V_2O_5 + 0.5Li^+ + 0.5e^- = \delta\text{-}LiV_2O_5 \quad (2)$$

$$\delta\text{-}LiV_2O_5 + Li^+ + e^- = \gamma\text{-}Li_2V_2O_5 \quad (3)$$

At a discharge–charge rate of 1.0 A g^{-1}, the carbon-coated V_2O_5 nanocrystals give rise to a total specific discharge capacity of approximately 297 mAh g^{-1} in the voltage range 2.0–4.0 V, very close to the theoretical capacity of 296 mAh g^{-1} for the formation of γ-$Li_2V_2O_5$ from the parent V_2O_5. During the charge process, a specific capacity of approximately 297 mAh g^{-1} is retained, demonstrating a Coulombic efficiency of nearly 100%. The high Coulombic efficiency indicates that, for the V_2O_5 nanocrystal material, the phase transition between δ-LiV_2O_5 and γ-$Li_2V_2O_5$ is highly reversible.

The carbon-coated V_2O_5 nanocrystals also show excellent rate capability (Figure 3). At current densities of 2.0, 5.0, and 10 A g^{-1} (rates of about 14C, 34C and 68C, respectively), the material still delivers discharge capacities of approximately 255, 168, and 130 mAh g^{-1}, respectively. To the best of our

dx.doi.org/10.1021/cm202812z | *Chem. Mater.* 2011, 23, 5290–5292

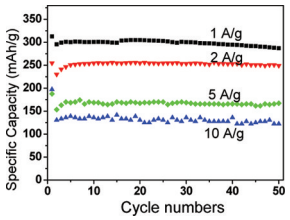

Figure 3. The cycling performance of the carbon-coated V_2O_5 nanocrystals at current densities of 1.0, 2.0, 5.0, and 10 A/g.

knowledge, the maximum value ever reported in the literature for the rate performance of V_2O_5 materials is 90 mAh g^{-1} at 40C (5.88 A g^{-1}).[19] More importantly, our V_2O_5 material also exhibits very high cycling stability. After discharge−charge cycles at 1.0 A g^{-1} for 50 cycles, a specific discharge capacity of approximately 288 mAh g^{-1} is still reached, accounting for a capacity fading between fifth and fiftieth cycles of only 2.7%. When cycling at 10 A g^{-1}, less than 2.3% discharge capacity fading is observed over 50 cycles. The electrochemical performance of the V_2O_5 nanocrystals is much superior over those of the micrometer-sized V_2O_5, V_2O_5 nanowires[20] (see Figure S4 in the Supporting Information), and other V_2O_5 nanomaterials reported in the literature.[4,9,19]

Scheme 2. Schematic Representation Showing the Structural Features of Carbon-Coated V_2O_5 Nanocrystals upon Li^+ Insertion/Extraction

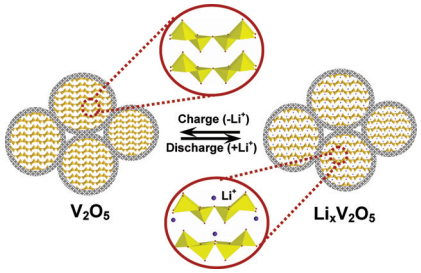

The impressive electrochemical performance of V_2O_5 nanocrystals is ascribed to its unique nanostructure (Scheme 2). The small particle size of V_2O_5 nanocrystals greatly shortens the diffusion and transport distance of lithium ions and electrons within the nanocrystals, whereas the voids among the nanocrystals provide fast transport pathways for the electrolyte and lithium ions. Furthermore, the thin layer of carbon formed during the decomposition of mesoporous carbon template partly covers the surface of the V_2O_5 nanocrystals, and the corresponding carbon-coating reduces the resistance of the interparticle boundary interfaces. As demonstrated by electrochemical impedance spectra (EIS), the consequent kinetics of lithium insertion/extraction is significantly improved (see Figure S5 in the Supporting Information). This carbon-coating not only improves the electrical conductivity of the electrode but also increases the stability of V_2O_5 material through reducing the surface reactions of the V_2O_5 nanocrystals with the electrolytes during charge−discharge cycling. As a result, the excellent rate capability and cycleability of V_2O_5 material are achieved.

In summary, a unique capillary-induction approach has been developed for the preparation of carbon-coated V_2O_5 nanocrystals. The combination of the particular morphology and carbon-coating leads the material to exhibit markedly enhanced specific discharge and charge capacities, excellent rate capability, and cycling stability. These merits make our material a promising candidate as a cathode material for high-performance lithium ion batteries. It is also feasible for our preparation technique to be scaled up for industrial application.

■ ASSOCIATED CONTENT

Ⓢ Supporting Information

Detailed experimental procedures, XRD patterns, TEM images of mesostructured carbon-V_2O_5 composite, and electrochemical performance and EIS spectra of micrometer-sized V_2O_5 and V_2O_5 nanowires. This material is available free of charge via the Internet at http://pubs.acs.org.

■ AUTHOR INFORMATION

Corresponding Author

*E-mail: k.wang@sjtu.edu.cn (K.W.); chemcj@sjtu.edu.cn (J.C.).

■ ACKNOWLEDGMENTS

This work was financially supported by the National Natural Science Foundation of China (20731003, 20901050), the National Basic Research Program of China (2011CB808703), and the Shanghai Pujiang Program (09PJ1405700).

■ REFERENCES

(1) Whittingham, M. S. *Chem. Rev.* **2004**, *104*, 4271.
(2) Kang, B.; Ceder, G. *Nature* **2009**, *458*, 190.
(3) Whittingham, M. S. *J. Electrochem. Soc.* **1975**, *122*, 713.
(4) Pan, A. Q.; Zhang, J. G.; Nie, Z. M.; Cao, G. Z.; Arey, B. W.; Li, G. S.; Liang, S. Q.; Liu, J. *J. Mater. Chem.* **2010**, *20*, 9193.
(5) Zhang, H. L.; Neilson, J. R.; Morse, D. E. *J. Phys. Chem. C* **2010**, *114*, 19550.
(6) Zhai, T. Y.; Liu, H. M.; Li, H. Q.; Fang, X. S.; Liao, M. Y.; Li, L.; Zhou, H. S.; Koide, Y.; Bando, Y.; Goberg, D. *Adv. Mater.* **2010**, *22*, 2547.
(7) Cao, A. M.; Hu, J. S.; Liang, H. P.; Wan, L. J. *Angew. Chem., Int. Ed.* **2005**, *44*, 4391.
(8) Li, X. X.; Li, W. Y.; Ma, H.; Chen, J. *J. Electrochem. Soc.* **2007**, *154*, A39.
(9) Mai, L. Q.; Xu, L.; Han, C. H.; Luo, Y. Z.; Zhao, S. Y.; Zhao, Y. L. *Nano Lett.* **2010**, *10*, 4750.
(10) Muster, J.; Kim, G. T.; Krstic, V.; Park, J. G.; Park, Y. W.; Roth, S.; Burghard, M. *Adv. Mater.* **2000**, *12*, 420.
(11) Wang, Y.; Cao, G. Z. *Chem. Mater.* **2006**, *18*, 2787.
(12) Chen, W.; Mai, L. Q.; Xu, Q.; Zhu, Q. Y.; Han, C. H.; Guo, W. L. *Solid State Ionics* **2003**, *161*, 205.
(13) Wang, Y. G.; Li, H. Q.; He, P.; Hosono, E.; Zhou, H. S. *Nanoscale* **2010**, *2*, 1294.
(14) Wang, Y. G.; Wang, Y. R.; Hosono, E. J.; Wang, K. X.; Zhou, H. S. *Angew. Chem., Int. Ed.* **2008**, *47*, 7461.
(15) Wu, X. L.; Jiang, L. Y.; Cao, F. F.; Guo, Y. G.; Wan, L. J. *Adv. Mater.* **2009**, *21*, 2710.
(16) Chou, S. L.; Wang, J. Z.; Sun, J. Z.; Wexler, D.; Forsyth, M.; Liu, H. K.; MacFarlane, D. R.; Dou, S. X. *Chem. Mater.* **2008**, *20*, 7044.
(17) Koltypin, M.; Pol, V.; Gedanken, A.; Aurbach, D. *J. Electrochem. Soc.* **2007**, *154*, A605.
(18) Meng, Y.; Gu, D.; Zhang, F. Q.; Shi, Y. F.; Yang, H. F.; Li, Z.; Yu, C. Z.; Tu, B.; Zhao, D. Y. *Angew. Chem., Int. Ed.* **2005**, *44*, 7053.
(19) Hu, Y. S.; Liu, X.; Muller, J. O.; Schlogl, R.; Maier, J.; Su, D. S. *Angew. Chem., Int. Ed.* **2009**, *48*, 210.
(20) Xiong, C. R.; Aliev, A. E.; Gnade, B.; Balkus, K. J. *ACS Nano* **2008**, *2*, 293.